Appl. Phys. A 76, 261–267 (2003)
DOI: 10.1007/s00339-002-1448-y
Applied Physics A
Materials Science & Processing

X. ZHANG[1,2,✉]
J. WEN[1]
C. SUN[1,2]

Thermal and carrier transport originating from photon recycling and non-radiative recombination in laser micromachining of GaAs thin films

[1] Department of Industrial and Manufacturing Engineering, The Pennsylvania State University, University Park, PA 16802, USA
[2] Department of Mechanical and Aerospace Engineering, University of California Los Angeles, Los Angeles, CA 90095, USA

Received: 24 January 2002/Accepted: 11 April 2002
Published online: 10 September 2002 • **© Springer-Verlag 2002**

ABSTRACT Coupled thermal and carrier transports (electron/hole generation, recombination, diffusion and drifting) in laser photoetching of GaAs thin film is investigated. A new volumetric heating mechanism originating from SRH (Shockley–Read–Hall) non-radiative recombination and photon recycling is proposed and modeled based on recent experimental findings. Both volumetric SRH heating and Joule heating are found to be important in the carrier transport, as well as the etching process. SRH heating and Joule heating are primarily confined within the space-charge region, which is about 20 nm from the GaAs surface. The surface temperature rises rapidly as the laser intensity exceeds 10^5 W/m^2. Below a laser intensity of 10^5 W/m^2, the thermal effect is negligible. The etch rate is found to be dependent on the competition between photovoltaic and photothermal effects on surface potential. At high laser intensity, the etch rate is increased by more than 100%, due to SRH and Joule heating.

PACS 44.10.+i; 72.40.+w; 73.61.Ey

1 Introduction

As direct-band-gap materials, III–V semiconductors have received a tremendous amount of interest from both the microelectronics industry and academia in the last decade since the realization of their promising applications in high-speed electronic devices and optoelectronics. In particular, commercialization of the semiconductor laser diode has demonstrated great potential in next-generation display technology. Recent advances in wide-band-gap GaN research shows an exciting potential in the realization of the blue semiconductor laser, a key step to achieving a full color display.

Effective process technologies such as etching and patterning are needed to fabricate compound devices. Currently, reactive ion etching (RIE) is used to etch the III–V semiconductor devices. However, there is a general concern with RIE because of the mechanical damage on the processed surface caused by the high-energy ion bombardment and because of the high process cost. Laser photoetching, as an alternative, provides a simple, low-cost and low-damage process since the "particles" used are "momentumless" photons [1, 2]. Laser wet etching has been used in various applications including microwave field effect transistors (FET), electrical depinning of GaAs and waveguides [3]. In order to develop laser wet etching as a viable process in device fabrication, accurate process control in laser wet etching needs to be achieved through a fundamental understanding of carrier and thermal/chemical transport in laser photoetching.

Laser photoetching is essentially a photo-electro-chemical process. Upon laser irradiation, photon-generated free carriers such as electrons and holes inside the semiconductor drift to the surface, and a substantial chemical reaction will take place at the semiconductor–liquid interface. The etching process involves three fundamental transports: free carrier transport, chemical reaction at interfaces and thermal transport. Carrier transport and chemical reaction in laser photoetching have been studied and modeled. Most previous studies claim that thermal transport is negligible because the radiative recombination of excited electrons and holes in III–V materials is a dominating mechanism due to the nature of the direct band gap [3, 4]. However, recent experiments on the minority carrier lifetime of n-type GaAs show evidence of significant Shockley–Read–Hall (SRH) non-radiative recombination and photon recycling [5]. Photon recycling refers to a continuous process in which radiative recombination from excited electrons and holes emits a new photon, which is again used for photoexcitation of a new electron/hole pair. With the combination of SRH non-radiative recombination and photon recycling during laser processing of III–V materials, the heat generation can be significant. The thermal transport originating from SRH non-radiative recombination of free carriers and its influence on the laser photoetching process, such as etch rate, should be therefore investigated.

In this work, coupled thermal and carrier transport in laser photoetching of GaAs is studied. A new heating mechanism based on SRH non-radiative recombination and photon recycling is proposed and modeled. Carrier generation, recombination, diffusion and drifting are numerically simulated, together with coupled thermal transport, including volumetric heat generation and thermal diffusion. The electrical and temperature field are modeled and subsequent influences on etching rate are calculated. A range of laser intensities will be investigated to explore the significance of the SRH and Joule heating in laser photoetching of GaAs thin films.

✉ Fax: +1-310/206-2302, E-mail: xiang@seas.ucla.edu

2 Fundamental mechanisms in laser photoetching of III–V semiconductors

2.1 *Thermal generation mechanisms in laser photoetching of III–V semiconductors*

Laser interaction with semiconductor materials is often characterized as an electron/hole excitation and recombination process. Upon laser irradiation, a valence electron can be excited by absorbing a photon, resulting in an electron in the conduction band and a hole in the valence band. The recombination of the excited electrons and holes depends on band structures. In indirect-band-gap materials such as silicon, excited electrons and holes undergo non-radiative recombination and the electronic energy is transferred to lattice vibrations (i.e. thermal energy). Thermal transport in the laser processing of indirect-band-gap materials is therefore a dominant process [6]. In direct-band-gap materials such as III–V semiconductors, there are three well-known recombination mechanisms (Fig. 1): (1) Radiative recombination, in which the excited electron and hole recombine and emit a photon [7]; (2) Shockley–Read–Hall (SRH) non-radiative recombination or thermal recombination via the recombination center, in which the electron and the hole recombine and release a phonon to the lattice (i.e. generate heat in the material) [8, 9]; and (3) Auger recombination, where the extra energy released by the electron and hole recombination will be absorbed by another nearby electron or hole [10]. It has been shown that the electron–hole recombination in GaAs is a radiative recombination dominant process [7, 10]. Thermal transport was not considered in previous work on the laser processing of GaAs materials.

In radiative recombination, the secondary photon generated from electron/hole-pair recombination is subsequently involved in the next event of electron/hole excitation, as shown in Fig. 1. This repeating process is often termed photon recycling [11, 12]. The thermal transport primarily results from SRH non-radiative recombination and photon recycling in laser interaction with direct-band-gap materials. Recent experiments on minority carrier lifetime in n-GaAs have indicated that SRH recombination is quite significant, even though the radiative process is still the dominant process in electron/hole recombination [5]. In laser photoetching of thin film GaAs grown on SiO_2 substrate, the SRH non-radiative recombination may lead to a significant temperature increase in the film due to the poor thermal conductivity of the substrate, which can greatly influence the carrier transport and etching process. In order to quantify the thermal transport in the laser etching of GaAs, an analysis is carried out in this work to determine the probability of SRH recombination in the whole recombination process, based on recent experimental findings [3].

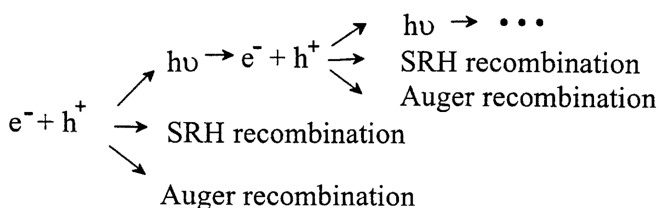

FIGURE 1 Photon recycling and SRH non-radiative recombination of carriers in laser interaction with n-GaAs: A new thermal mechanism originating from SRH non-radiative recombination

The dynamic recombination of the electron/hole-pair after photon excitation can be described by the following differential equation:

$$\frac{dN}{dt} = -\lambda (N - N_0) , \tag{1}$$

where N is the number density of the carriers, N_0 is the number density of carriers at equilibrium, and $1/\lambda = \tau$ is the lifetime of the carriers. Since the recombination has several channels, the recombination can be represented in the following form:

$$\frac{dN}{dt} = -\left(\lambda_{\text{radiative}} + \lambda_{\text{Auger}} + \lambda_{\text{SRH}}\right)(N - N_0) . \tag{2a}$$

In the experiment conducted by Luch et al., the lifetime τ_{DH} of minority carriers was measured by the photoluminescence (PL) in the double heterostructure (DH) GaAs [5]:

$$\frac{1}{\tau_{DH}} = \frac{1}{\tau_{\text{radiative}}} + \frac{1}{\tau_{SRH}} + \frac{1}{\tau_{\text{Auger}}} . \tag{2b}$$

The objective here is to calculate the $\tau_{\text{radiative}}$ and τ_{SRH} as bulk properties from the measured τ_{DH} in the experiment by Luch et al. [5].

With the DH structure, the photoluminescence (PL) decay in GaAs material is independent of diffusion; thus the lifetime deduced from the experimental results can be regarded as the local property of the material. The measured PL lifetime τ_{DH} can be represented as:

$$\frac{1}{\tau_{DH}} = \frac{1}{\tau_{\text{bulk}}} + 2\frac{S}{w} , \tag{3}$$

where S is the average value of recombination velocities at the front and back interfaces, and w is the thickness of the active layer. The non-linear dependence of $\frac{1}{\tau_{DH}}$ on $\frac{1}{w}$ from the experimental results indicates that photon recycling occurs during photoluminescence decay, causing $\frac{1}{\tau_{\text{bulk}}}$ and S to vary with the thickness of the active layer.

It has been concluded from the analysis of the PL data that S is very small and $\frac{2S}{w}$ was negligible, which yields the following:

$$\frac{1}{\tau_{DH}} \approx \frac{1}{\tau_{\text{bulk}}} = \frac{1}{\tau_{\text{radiative}}} + \frac{1}{\tau_{SRH}} + \frac{1}{\tau_{\text{Auger}}} . \tag{4}$$

From further analysis of the photoluminescence (PL) experiment, Luch et al. concluded that the Auger recombination is negligible:

$$\frac{1}{\tau_{DH}} \approx \frac{1}{\tau_{\text{radiative}}} + \frac{1}{\tau_{SRH}} . \tag{5}$$

Considering the photon recycling effect in the DH structure, the photon recycling factor ϕ is introduced, which varies with w, the thickness of the active layer:

$$\frac{1}{\tau_{DH}} \approx \frac{1}{\phi\tau_{\text{radiative}}} + \frac{1}{\tau_{SRH}} . \tag{6}$$

The dependence of τ_{DH} on w directly results from the $\phi(w)$, while $\tau_{radiative}$ and τ_{SRH} are considered as bulk material properties without photon recycling. $\phi(w)$ was obtained from a theoretical model [11] and $\tau_{DH}(w)$ was measured from PL experiments [5]. $\tau_{radiative}$ and τ_{SRH} are then determined in this work by fitting the $\tau_{DH}(w)$ with $\phi(w)$, using the least-square method for each doping level. It is found that $\tau_{radiative} = 6.24\,\text{ns}$; $\tau_{SRH} = 24.78\,\text{ns}$ at a doping level of $10^{18}/\text{cm}^3$ in n-GaAs. The SRH recombination probability η, can therefore be expressed as:

$$\eta = \frac{\tau_{radiative}}{\tau_{radiative} + \tau_{SRH}} = 0.201\,. \tag{7}$$

This indicates that about 20% of the electron/hole pairs recombine through SRH non-radiative recombination. Thermal energy transfer is therefore quite significant in the laser photoetching of GaAs thin film. Volumetric SRH heating g_{SRH} can be described by following:

$$g_{SRH} = \frac{(p - p_0)}{\tau_{SRH}} E_g\,. \tag{8a}$$

E_g is the band gap and p is the minority carrier concentration at a specific location (p_0 is a thermal equilibrium concentration). Joule heating, in contrast, originates from carrier flow as:

$$g_j = -J\frac{\partial \phi}{\partial z} \tag{8b}$$

where J is the total current including both electrons and holes.

2.2 *Physical and chemical processes in laser wet photoetching of n-GaAs*

In laser wet photoetching, the immersed n-GaAs film has a different Fermi level from its surrounding electrolytic solution (Fig. 2) [5]. As a result of the chemical potential difference, the electrons flow across the interface between the GaAs thin film and the solution, resulting in the formation of a space-charge region in GaAs and band bending near the surface. The band bending introduces an electric field that reduces further electron flow to the solution and favors hole migration to the solution. In the absence of laser light, the hole concentration is not sufficient to induce a measurable etching.

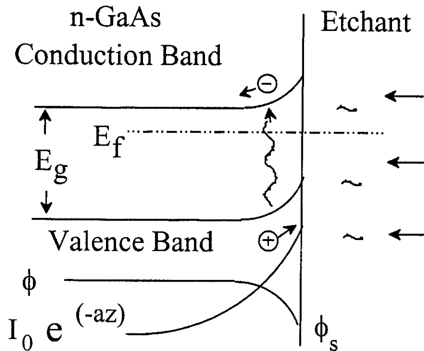

FIGURE 2 Physical processes in laser photoetching of n-GaAs thin films: optical absorption, electron and hole photoexcitation, recombination, diffusion, band bending and drifting

Upon laser irradiation, a large quantity of holes is generated in the valence band and drifts to the surface by the electric field in the space-charge region. The etching of GaAs is essentially an electrochemical anodic dissolution process [13]. The surface Ga and As atoms are triply bonded to each other and the lower atoms by valence electrons. Once a hole drifts to the surface and is captured by one of the valence bonds, the bond is broken, leaving one unpaired electron with an As atom, while the positively charged Ga ion is matched by a negatively charged nucleophilic agent from the electrolytic solution. Since the energy level of the unpaired electron in the As atom is close to that of the valence band, it is likely that the As atom captures another hole to form a positively charged ion, which will in turn be matched by another nucleophilic agent. Two holes are consumed to break one valence bond between Ga and As atoms. For the dissolution of a GaAs cell, six holes are needed in total. The laser photoetching etch rate can therefore be calculated by the hole flux at the GaAs surface.

Under laser irradiation, the photoexcited electrons and holes are transported by several mechanisms in GaAs (Fig. 2) [4]. Firstly, free electrons and holes are generated by the laser photon excitation. The electron and hole concentrations strongly depend on the optical absorption profile in the GaAs, which is a function of the laser wavelength. Secondly, free electrons and holes recombine within the GaAs film via three routes: radiative recombination, SRH non-radiative recombination and Auger recombination. Photon recycling occurs simultaneously with the recombination processes. Thirdly, under the electric field in the space-charge region, the electrons drift away from the interface while the holes drift towards the interface. Finally, the electrons and holes diffuse into the thin film, due to the carrier concentration gradients established by laser absorption in GaAs.

The electron and hole transport is strongly coupled with the thermal transport that originates from volumetric SRH heating and Joule heating. Carrier generation, diffusion and drifting result in a carrier distribution profile and flux within the film, and therefore determine the electron–hole recombination rate (i.e. volumetric SRH heating and Joule heating). The temperature increase in the GaAs film due to thermal conduction, in turn, influences the carrier transport and surface potential distribution, which dictates the carrier transport in the space-charge region. The complex coupled thermal and carrier transports eventually determine the hole flux to the surface and laser photoetching rate in GaAs thin films.

3 Numerical modeling

In this work, the CW argon laser ($\lambda = 488\,\text{nm}$) photoetching of a n-GaAs film grown on a SiO_2 substrate is numerically investigated (Fig. 3). The mathematical description of laser photoetching of the GaAs thin film consists of two parts: the carrier transport equation set for the electron and hole generation, recombination, drifting and diffusion in the GaAs thin film, and the thermal transport equation with the SRH heating and Joule heating. A one-dimensional model is used to investigate the coupled carrier and thermal transports since the laser beam size is typically much larger than the thickness of the GaAs thin film. Only thermal conduction is considered at this point, with the goal

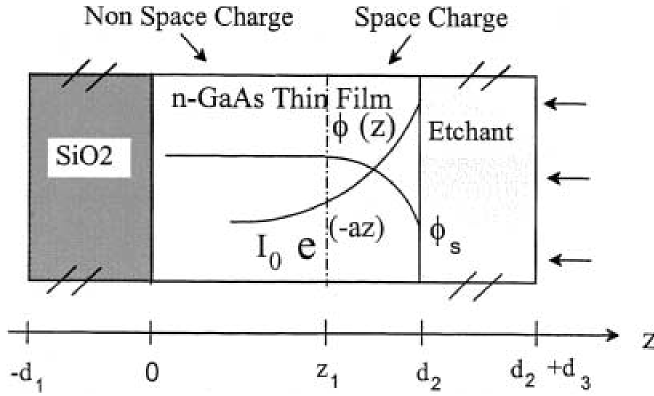

FIGURE 3 Schematic diagram of the 1D substrate–GaAs thin film–solution system. The thin film consists of two regions: a space-charge region and a non-space-charge region

of extracting important physical characteristics in laser photoetching of the GaAs thin film. The physical and chemical parameters used in the numerical simulation are given in Table 1.

For thermal transport, the 1D system is divided into three regions: the SiO_2 substrate, the GaAs thin film and the electrolytic solution.

$$\varrho C\frac{\partial T}{\partial t}=\frac{\partial}{\partial z}\left(k\frac{\partial T}{\partial z}\right)+g \tag{9}$$

where $g=g_{\mathrm{SRH}}+g_{\mathrm{J}}$, the sum of volumetric SRH heating, g_{SRH}, and Joule heating, g_{J}, which are defined in (8). g is set to zero for the substrate and solution. The initial condition and boundary conditions are given as follows:

$$\begin{aligned}T(z,t=0)&=T_0\\T(z=-d_1,t)&=T_0\\T(z=d_2+d_3,t)&=T_0\,.\end{aligned} \tag{10}$$

Here d_1, d_2, and d_3 represent the thickness of SiO_2 substrate, GaAs thin film and electrolytic solution, respectively, as shown in Fig. 3.

A general form of electron and hole transport including carrier generation, recombination, diffusion and drifting can be expressed as [4, 14]:

Poisson equation:

$$\nabla^2\phi+\frac{\mathrm{e}}{\varepsilon\varepsilon_0}(p-n+N_{\mathrm{d}}-N_{\mathrm{a}})=0 \tag{11}$$

Electron transport:

$$\frac{1}{\mathrm{e}}\frac{\partial \boldsymbol{J}_n}{\partial z}+\frac{\alpha I_0\,\mathrm{e}^{-\alpha z}}{h\nu}-\frac{p-p_0}{\tau}=0 \tag{12}$$

Hole transport:

$$-\frac{1}{\mathrm{e}}\frac{\partial \boldsymbol{J}_p}{\partial z}+\frac{\alpha I_0\,\mathrm{e}^{-\alpha z}}{h\nu}-\frac{p-p_0}{\tau}=0\,. \tag{13}$$

$\boldsymbol{J}_n=kT\mu_n\frac{\partial n}{\partial z}-\mathrm{e}\mu_n n\frac{\partial\phi}{\partial z}$, $\boldsymbol{J}_p=-kT\mu_p\frac{\partial p}{\partial z}-\mathrm{e}\mu_p p\frac{\partial\phi}{\partial z}$ are electron and hole current densities, respectively, including diffusion and drifting terms. The Einstein relationship between the carrier mobility and diffusion constant of charge d particles is used [15]: $D=\frac{kT}{q}\mu$ Carrier transport is investigated in two regions within the GaAs films: a non-space-charge region (NSC) where the drifting term is zero due to the lack of an electric field, and a space-charge region (SC) where the drifting term is non-zero. Boundary conditions are given as follows:

in the NSC region:

Hole:

$$\begin{aligned}&p(z=0,t)=p_0(T_0)\\&D_p\left.\frac{\partial p}{\partial z}\right|_{z=z_1}=\frac{J_p'}{\mathrm{e}}\end{aligned} \tag{14}$$

Electron:

$$\begin{aligned}&n(z=0,t)=N_{\mathrm{D}}\\&D_n\left.\frac{\partial n}{\partial z}\right|_{z=z_1}=\frac{J_n'}{\mathrm{e}}\end{aligned} \tag{15}$$

In the SC region:

Hole:

$$\begin{aligned}&J_p(z=z_1)=J_p'\\&J_p(z=d_2)=Kp(z=d_2)\end{aligned} \tag{16}$$

Electron:

$$\begin{aligned}&J_n(z=z_1)=J_n'\\&J_n(z=d_2)=Kn(z=d_2)\end{aligned} \tag{17}$$

Potential:

$$\begin{aligned}&\Phi(z=z_1)=0\\&\Phi(z=d_2)=-0.5\left(\frac{T}{T_0}\right)+\frac{kT}{\mathrm{e}}\ln\left(\frac{I}{I_c}\right)\end{aligned} \tag{18}$$

SiO_2:	$\varrho=2.2\times10^3$ kg/m^3 $C=740.0$ J/kg/K $k=1.39$ W/m/K	hole diffusivity: $D_{\mathrm{p}}=4.0\times10^{-4}$ m^2/s electron diffusivity: $D_{\mathrm{n}}=222.0\times10^{-4}$ m^2/s optical absorption coefficient ($\lambda=488$ nm) $\alpha=1.117\times10^7$ m^{-1}
GaAs:	$\varrho=5.3168\times10^3$ kg/m^3 $C=(343.0+4.7\times10^{-2}T-3.2\times10^6/T^2)$ J/kg/K $k=(7.45\times10^4/T^{1.3})$ W/m/K	Planck Constant: $h=6.63\times10^{-34}$ J s Boltzmann Constant: $k=1.38\times10^{-23}$ J/K mass of electron: $m_{\mathrm{e}}=9.1\times10^{-31}$ kg
Solution:	$\varrho=1.0\times10^3$ kg/m^3 $C=4.1868\times10^3$ J/kg/K $k=0.6$ W/m/K	band gap of GaAs: $E_{\mathrm{g}}=1.5$ eV $=2.4\times10^{-19}$ J doping concentration: $N_{\mathrm{D}}=1.0\times10^{18}$ cm^{-3}

TABLE 1 Physical properties and parameters used in numerical modeling

Here, z_1 is the thickness of the NSC region and J'_n, J'_p represent the current densities at the interface z_1 between the NSC and SC regions. The surface potential dependence on laser intensity was measured in earlier work [16, 17]. One-dimensional coupled thermal and carrier transport equations were solved numerically by the finite-difference method [18, 19]. The temperature and carrier concentrations were investigated spatially and temporally. The etch rate dependence on laser intensity was therefore obtained.

4 Results and discussions

Laser-induced electric potential distribution in the space-charge region was calculated for two laser intensities, $I = 10^6$ and 10^7 W/m^2, at timescales of 10 ms and 3 s, respectively (Fig. 4). At the timescale of 3 s, the potential reached a steady state as the temperature reached a steady state, which will be discussed in Fig. 7. It is found that this space-charge region is about 20 nm below the GaAs film surface and the surface potential is less than 1 V. At a short timescale, such as 10 ms, the potential induced by higher laser intensity is higher than that of a lower laser intensity, indicating that the laser-induced band flattens near the surface (Fig. 4). With increasing irradiation time, the potential is decreased within the space-charge region for both laser intensities, suggesting band bending near the surface. The potential drop at higher laser intensity from 10 ms to 3 s is much larger than that at a lower laser intensity, as shown in Fig. 4. This can be explained by the surface potential dependence on temperature and laser intensity (18). At the short timescale of 10 ms, the laser intensity becomes a dominant factor for the surface potential ϕ_s (18) since the increase in temperature of the GaAs thin film is negligible, as demonstrated in the next section. The surface potential ϕ_s increases with increasing laser intensity I, resulting in band flattening near the surface. With the continuous irradiation of the laser beam on the GaAs thin film, the temperature starts to rise in the space-charge region, which leads to a decrease in the surface potentials, or band bending, as the $\ln(I/I_0)$ term is generally negative for the laser intensity relevant to practical processes (i.e. $I < I_0$). The thermally induced band bending is clearly seen for the higher intensity of 10^7 W/m^2 at 3 s (Fig. 4). The competition between photothermal band bending and photovoltaic band flattening is also observed, which is discussed later.

As the laser photoetching of n-GaAs thin film is dominated by the electron and hole transport within the film and hole flux at the interface between the thin film and solution, electron and hole concentration distributions in both the space-charge region and the non-space-charge region were investigated. Fig. 5 shows the steady-state electron and hole distributions in the space-charge region close to the interface at laser intensities of 10^6 and 10^7 W/m^2. The electron concentration decreases dramatically (4–6 orders) near the surface, while hole concentration increases greatly due to the strong electric field from the potential drop (Fig. 4) in the space-charge region. It is seen that the lower laser intensity generates lower carrier concentrations near the surface. Minority carrier inversions are observed at both laser intensities. In the n-GaAs thin film at thermal equilibrium, holes are generally considered to be a minority carrier whose concentration is smaller than that of the majority carrier electrons. However, the optical excitation in laser etching of n-GaAs generates a much larger quantity of electrons and holes than does thermal excitation. Initially, the concentration of laser-generated electrons and holes is quite similar to the optical absorption profile in the film (i.e. the carrier concentration decreases exponentially from the surface of the film into its depths). Under multiple transport mechanisms such as diffusion, drifting and recombination, the electrons and the holes are distributed quite differently from their initial concentration. Within the space-charge region, the hole concentration increases dramatically due to drifting under the strong electrical field, causing the hole concentration to exceed the electron concentration at a depth of 10 nm from the surface, and therefore the hole becomes a majority carrier. The minority carrier inversion has a significant effect on the carrier recombination as well as the volumetric SRH heating.

It has been found that the Joule heating is confined to a region of a few nanometers near the interface (Fig. 6). This is because the high carrier flux density occurs very close to the surface due to the dramatic potential drop in the region. Distribution of the SRH heating, in contrast, has a peak located a little farther from the surface compared with that of the Joule

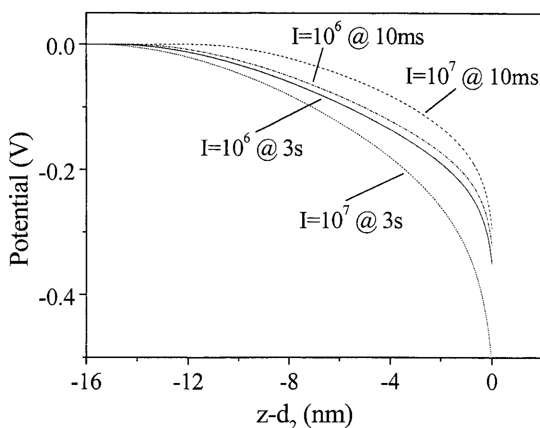

FIGURE 4 Potential distribution within the space-charge region for two laser intensities 10^6 and 10^7 W/m^2 at 10 ms and 3 s

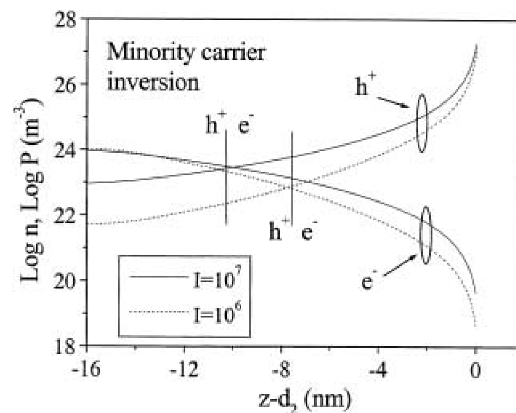

FIGURE 5 Electron and hole concentration distributions within the space-charge region for two laser intensities 10^6 and 10^7 W/m^2. Minority carrier inversion occurs for both laser intensities

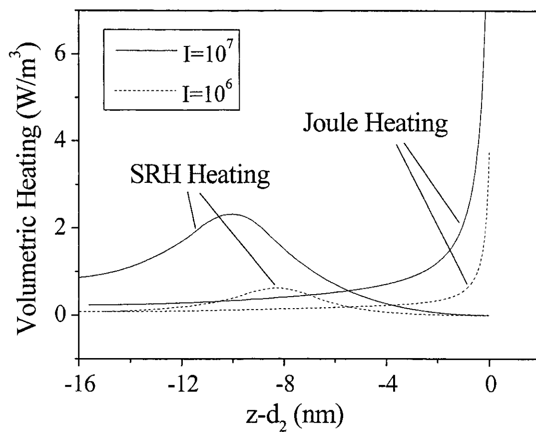

FIGURE 6 Volumetric SRH heating and Joule heating during the laser etching of n-GaAs thin films at two laser intensities, 10^6 and 10^7 W/m^2

heating. This peak originates from the minority carrier inversion where the minority carrier concentration reaches the maximum at the inversion point. The volumetric Joule heating and SRH heating are found to have a similar order of magnitude and are primarily confined to the space-charge region. Therefore, it is important to consider both of these thermal mechanisms in the laser etching of GaAs thin films. Since both SRH and Joule heating are confined within 20 nm of the surface, a non-uniform temperature distribution is expected if the heat cannot dissipate efficiently within a short time. However, this work shows that at a timescale beyond ms, the heat can be conducted efficiently through the n-GaAs film and the temperature distribution is almost uniform across the film.

Transient surface temperature in laser photoetching of n-GaAs thin film was studied and the steady-state surface temperature could be reached in a timescale of seconds for laser intensities of 10^6 W/m^2 and 10^7 W/m^2 (Fig. 7a). It was found that the induced surface temperature strongly depended on laser intensity. The temperature could be substantially high, 593 K at 10^7 W/m^2, compared with 330 K at 10^6 W/m^2. High laser intensity created a higher concentration of carriers and carrier fluxes in the space-charge region. Both Joule heating and SRH non-radiative heating were enhanced by higher carrier concentrations and fluxes, leading to a higher surface temperature. It was also observed that the surface temperature increased significantly only after the laser intensity reached more than 10^6 W/m^2. Below the laser intensity of 10^5 W/m^2, the temperature increase was negligible, which is consistent with previous experiments at lower laser intensities [3]. This threshold behavior results from the competition among photon excitation, electron/hole diffusion, drifting and recombination and photon recycling. It should be pointed out here that, at the high laser intensity of 10^7 W/m^2, the assumption that there is only conduction heat transfer through the etchant is no longer accurate since there may be boiling and related two-phase heat transfer and fluid flow in the etchant solution. Though this work focuses on revealing the RSH and photon recycling heating effects on photo micromachining, future work will be needed to address surface-heating-induced two-phase heat transfer and fluid flow at high laser intensity.

As an important practical parameter, etch rate in laser photoetching of n-GaAs thin films was numerically investigated

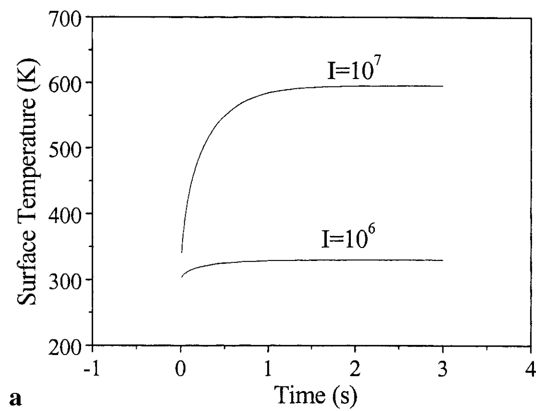

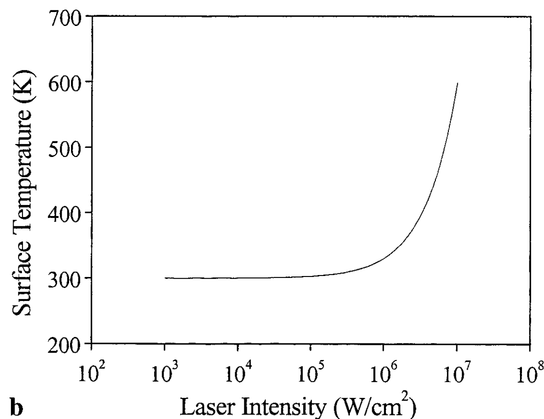

FIGURE 7 Transient surface temperature during laser photoetching of n-GaAs thin film (**a**), and temperature dependence on laser intensity (**b**)

by resolving coupled thermal and carrier transports. The etch rate was found to be a strong function of the laser intensity (Fig. 8). In principle, etch rate is determined by the hole flux at the GaAs surface, which is largely dictated by the photon-excited free carriers and the transport of these carriers through both the non-space charged and the space-charge regions. Higher laser intensity results in higher hole flux at the surface, and therefore a higher etch rate. It has been found that, at laser intensities below 10^5 W/m^2, the etch rate increases almost linearly with the laser intensity. In the low laser intensity range, the photon-excited free carriers are proportional to the laser intensity such that the etch rate is linearly dependent on laser intensity. This suggests that band flattening at low laser intensity may not play a significant role in carrier transport, although it is expected to reduce the hole flux to the surface. It should be stressed that the band flattening affects the overall transport in a complex way. As the laser intensity is increased above 10^5 W/m^2, the etch rate increase slows down and tends to be saturated. In this range, the electronic band bending is further flattened and the surface potential increases from -0.5 V to $-0.4/-0.35$ V. The hole flux drift to the surface is effectively reduced due to this band flattening, slowing down the increase in the etch rate, as seen in Fig. 8.

In order to understand how SRH heating and Joule heating influence the etch rate, the etch-rate dependence on laser intensity calculated from coupled thermal and carrier transports is compared with that calculated by considering carrier transport only (Fig. 8). It has been found that, at a laser in-

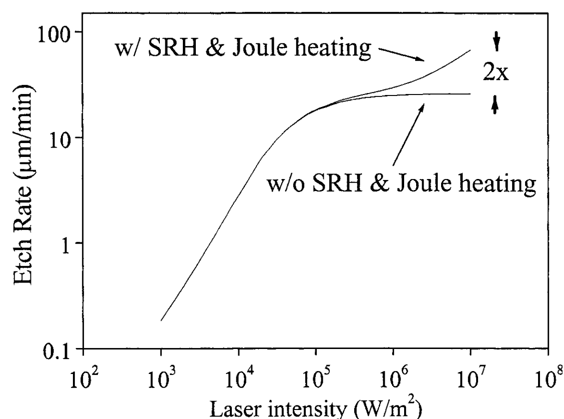

FIGURE 8 Photo etch rate dependence on the laser intensity

tensity below 10^5 W/m^2, the etch rate calculated with the thermal consideration is almost the same as that calculated without the thermal consideration. This is because the photovoltaic mechanism dominates the surface potential at the low-intensity range since the temperature rise in the film is very small (Fig. 9). As the intensity increases above 10^5 W/m^2, the etch rate calculated with the thermal consideration becomes higher than that calculated without the thermal consideration. At a laser intensity of 10^7 W/m^2, the etch rate with the thermal consideration is about two-times higher than that without the thermal consideration. The significant difference in the etch rate is explained by the photothermal effect on the surface band bending at high laser intensities, shown in Fig. 9. When the laser intensity increases above 10^5 W/m^2, the temperature in the n-GaAs film increases rapidly, as seen in Fig. 7b. The temperature increase effectively reduces the surface potential (18), resulting in a higher degree of band bending (Fig. 9). The photothermal-induced band bending favors the hole drift to the surface, leading to a higher etch rate. In contrast, without considering SRH heating and Joule heating, further flattening of the band with the increase in laser intensity reduces the hole flux to the surface and saturates the etch rate, as seen in Fig. 8. It was demonstrated that the etch rate dependence on the laser intensity depends strongly on the competition between photovoltaic and photothermal effects on the surface potential.

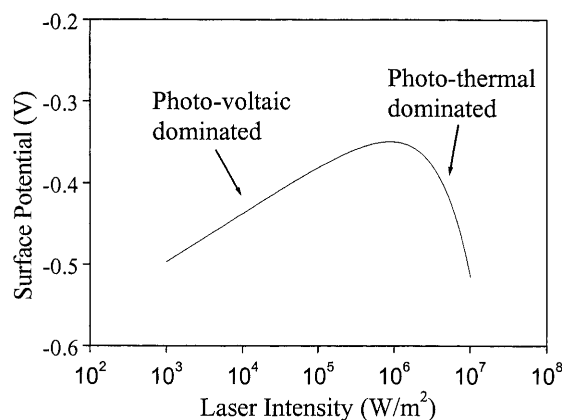

FIGURE 9 Surface potential dependence on laser intensity: the competition between photothermal and photovoltaic effects on band bending

5 Conclusions

Coupled thermal and carrier transports in laser photoetching of n-GaAs thin film have been investigated. A new thermal mechanism based on SRH non-radiative recombination and photon recycling has been proposed and modeled. Laser carrier generation, recombination, diffusion and drifting have been numerically modeled, together with the heat transport arising from SRH heating and Joule heating. It was found that volumetric SRH heating and Joule heating are confined to the space-charge region, which is about 20 nm from the surface, and have the same order of magnitude. The surface temperature rises significantly as the laser intensity exceeds 10^5 W/m^2 to 593 K at 10^7 W/m^2. Electron and hole concentrations and the electric potential distribution in the space-charge region have been simulated. Band flattening at high laser intensity and band bending with the increase in the surface temperature at high laser intensity are observed. The competition between photovoltaic and photothermal effects on the surface potential and band bending determines the dependence of the etch rate on the laser intensity.

ACKNOWLEDGEMENTS This project is supported by the National Science Foundation CAREER Award No. DMI 9703426 and the Office of Naval Research (ONR) Young Investigator Award, Grant No. N00014-99-1-0492.

REFERENCES

1 M.S. Minsky, M. White, E.L. Hu: Appl. Phys. Lett. **68**, 1531 (1996)
2 M.K. Kelly, O. Ambacher, B. Danlheimer, G. Gross, H. Angerer, M. Stutzmann: Appl. Phys. Lett. **69**, 1749 (1996)
3 M.N. Ruberto, X. Zhang, R. Scarmozzino, A.E. Willner, D.V. Podlesnik, R.M. Osgood Jr.: J. Electrochem. Soc. **138**, 1174 (1991)
4 E. Mannheim, R.C. Alkire, R.L. Sani: J. Electrochem. Soc. **141**, 546 (1994)
5 G.B. Luch, H.F. MacMillan, M.R. Melloch, R.K. Ahrenkiel, M.S. Lundstorm: J. Appl. Phys. **72**, 1436 (1992)
6 H.L. Douglas, G.E. Jellison Jr., R.F. Wood: Phys. Rev. B **26**, 6747 (1982)
7 S.M. Sze: *Physics of Semiconductor Devices* (Wiley, New York 1981)
8 W. Shockley, W.T. Read Jr.: Phys. Rev. **87**, 835 (1952)
9 R.N. Hall: Phys. Rev. **87**, 835 (1952)
10 J. Gowar: *Optical Communication Systems* (Prentice Hall, London 1984)
11 R.K. Ahrenkiel, D.J. Dunlavy, B. Keyes, S.M. Vernon, T.M. Dixon, S.P. Tobin, K.L. Miller, R.E. Hayes: Appl. Phys. Lett. **55**, 1088 (1989)
12 P. Asbeck: J. Appl. Phys. **48**, 820 (1977)
13 P.H.L. Notten, J.E.A.M. van den Meerakker, J.J. Kelly: *Etching of III–V Semiconductors, An Electrochemical Approach* (Elsevier Advanced Technology, United Kingdom 1991)
14 F.W. Ostermayer Jr., P.A. Kohl, R.M. Lum: J. Appl. Phys. **58**, 4390 (1985)
15 V.S. Bagotzky: *Fundamentals of Electrochemistry* (Plenum Press, New York, London 1993)
16 M.E. Orazem, J. Newman: In *Modern Aspects of Electrochemistry*, Vol. 18, ed. by R.E. White, B.E. Conway, J. O'M. Bockris (Plenum Press, New York, London 1986)
17 F. Kuhn-Kuhnenfeld: J. Electrochem. Soc.: Solid State Sci. Technol. **119**, 1063 (1972)
18 M. Kurata: *Numerical Analysis for Semiconductor Devices* (Lexington books, Lexington, Massachusetts 1982)
19 D.L. Scharfetter, H.K. Gummel: IEEE Trans. Electron Devices **16**, 64 (1969)